

ARMY RESEARCH LABORATORY

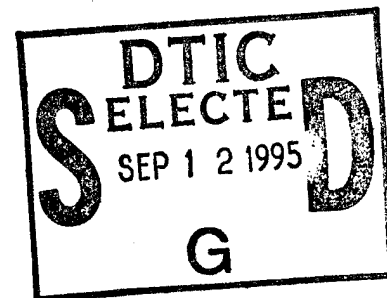


Roll Damping for Finned Projectiles Including: Wraparound, Offset, and Arbitrary Number of Fins

Ameer G. Mikhail

ARL-TR-846

August 1995



19950911 015

APPROVED FOR PUBLIC RELEASE; DISTRIBUTION IS UNLIMITED.

DTIC QUALITY INSPECTED 8

NOTICES

Destroy this report when it is no longer needed. DO NOT return it to the originator.

Additional copies of this report may be obtained from the National Technical Information Service, U.S. Department of Commerce, 5285 Port Royal Road, Springfield, VA 22161.

The findings of this report are not to be construed as an official Department of the Army position, unless so designated by other authorized documents.

The use of trade names or manufacturers' names in this report does not constitute indorsement of any commercial product.

REPORT DOCUMENTATION PAGE

Form Approved
OMB No. 0704-0188

Public reporting burden for this collection of information is estimated to average 1 hour per response, including the time for reviewing instructions, searching existing data sources, gathering and maintaining the data needed, and completing and reviewing the collection of information. Send comments regarding this burden estimate or any other aspect of this collection of information, including suggestions for reducing this burden, to Washington Headquarters Services, Directorate for Information Operations and Reports, 1215 Jefferson Davis Highway, Suite 1204, Arlington, VA 22202-4302, and to the Office of Management and Budget, Paperwork Reduction Project(0704-0188), Washington, DC 20503.

1. AGENCY USE ONLY (Leave blank)		2. REPORT DATE August 1995	3. REPORT TYPE AND DATES COVERED Final, January 1992 - May 1993	
4. TITLE AND SUBTITLE Roll Damping for Finned Projectiles Including: Wraparound, Offset, and Arbitrary Number of Fins			5. FUNDING NUMBERS 1L162618AH80 62618A-00-001 AJ	
6. AUTHOR(S) Ameer Mikhail				
7. PERFORMING ORGANIZATION NAME(S) AND ADDRESS(ES) US Army Research Laboratory ATTN: AMSRL-WT-PB Aberdeen Proving Ground, MD 21005-5066			8. PERFORMING ORGANIZATION REPORT NUMBER ARL-TR-846	
9. SPONSORING/MONITORING AGENCY NAMES(S) AND ADDRESS(ES)			10. SPONSORING/MONITORING AGENCY REPORT NUMBER	
11. SUPPLEMENTARY NOTES				
12a. DISTRIBUTION/AVAILABILITY STATEMENT Approved for public release; distribution is unlimited.			12b. DISTRIBUTION CODE	
13. ABSTRACT (Maximum 200 words) An algebraic correlation for the roll-damping and roll-producing moments coefficients for finned projectiles and missiles has been extended and verified to accept 1) bodies with arbitrary number of fins (i.e., not only four cruciform fins), 2) curved wraparound fins with fin cant, and 3) fins with offset angles. The extended correlation is also applicable in subsonic, transonic, and supersonic speed regimes. A direct method to compute the fin roll-producing moment from the fin normal force is provided to circumvent the lengthy and cumbersome semi-empirical existing methods. Seven different missile and projectile configurations with widely varying fin shapes and sizes were tested, and their measured data are provided for completeness. The present correlation is very simple and can be used to refine initial configuration selection and thus reduces the number of costly full flow field computations.				
14. SUBJECT TERMS projectiles, aerodynamics, fins, roll motion, damping, correlation, prediction, missiles, supersonic, transonic, subsonic			15. NUMBER OF PAGES 35	
			16. PRICE CODE	
17. SECURITY CLASSIFICATION OF REPORT UNCLASSIFIED	18. SECURITY CLASSIFICATION OF THIS PAGE UNCLASSIFIED	19. SECURITY CLASSIFICATION OF ABSTRACT UNCLASSIFIED	20. LIMITATION OF ABSTRACT SAR	

INTENTIONALLY LEFT BLANK.

TABLE OF CONTENTS

	<u>Page</u>
LIST OF FIGURES	v
LIST OF TABLES	vii
1. INTRODUCTION	1
2. ANALYSIS	2
2.1 The Pure Rolling Motion Equation	2
2.1.1 The Cant Angle and Equivalent Cant Angle	2
2.2 The Correlation of Eastman	3
2.3 Extension to an Arbitrary Number of Fins	3
2.4 Extension to Curved, Canted Wraparound Fins	4
2.5 Extension to Projectiles With Offset Fins	4
2.6 Fast Evaluation of C_{ls}	5
3. RESULTS OF APPLICATION TO DIFFERENT CONFIGURATIONS	6
3.1 The M829 Kinetic Energy Projectile (Arbitrary Number of Fins)	6
3.2 The HYDRA 70-mm MK66 Army Missile (Curved Wraparound and Arbitrary Number of Fins)	6
3.3 The BRL Research Projectile (Offset Fins)	7
3.4 The Terrier-Recruit First-Stage Vehicle	8
3.5 The GSRS Boeing Rocket	9
3.6 The Air Force 2.75-Inch (70mm-m) Folding Fin Rocket	10
3.7 The Basic Finner Configuration	10
4. SUMMARY AND CONCLUSIONS	12
5. REFERENCES	25
LIST OF SYMBOLS	27

Accession For	
NTIS CRA&I	<input checked="" type="checkbox"/>
DTIC TAB	<input type="checkbox"/>
Unannounced	<input type="checkbox"/>
Justification _____	
By _____	
Distribution / _____	
Availability Codes	
Dist	Avail and/or Special
A-1	

INTENTIONALLY LEFT BLANK.

LIST OF FIGURES

<u>Figure</u>		<u>Page</u>
1	Nomenclature for fin arrangements.	13
2	Fin cant (deflection) angle, δ	14
3	Nomenclature for estimating $C_{l\delta}$ from C_N	15
4	Geometry, validation, and application to the M829 Kinetic Energy projectile. .	16
5	Geometry, validation, and application to the HYDRA 70mm MK66 missile. . .	17
6	Geometry, validation, and application to the BRL Research Projectile.	18
7	Geometry, validation, and application to the Terrier- Recruit first stage vehicle.	19
8	Geometry, validation, and application to Boeing GSRS.	20
9	Geometry, validation, and application to the Air Force 2.75 inch (70mm) rocket.	21
10	Geometry, validation, and application to the Tri-Service Basic Finner projectile.	22
11	Comparison for C_{lp} computed by different methods.	23
12	Compilation of all data of all configurations	24

INTENTIONALLY LEFT BLANK.

LIST OF TABLES

<u>Table</u>		<u>Page</u>
1	Data and Results for the M829 Projectile	6
2	Data and Results for the HYDRA 70-mm MK66	7
3	Data and Results for the BRL Research Projectile	8
4	Data and Results for the Terrier-Recruit First-Stage Vehicle	9
5	Data and Results for the GSRS Boeing Rocket	9
6	Data and Results for the AF 2.75-inch Rocket	10
7	Data And Results for the Basic Finner Projectile	11

INTENTIONALLY LEFT BLANK.

1. INTRODUCTION

The roll-damping coefficient is needed to compute the rolling motion and history and to estimate the steady-state spin rate for projectiles and missiles. One also needs to know the corresponding fin-produced roll moment coefficient, $C_{l\delta}$, which is relatively easier to measure in wind tunnels or compute with analytic and empirical formulae. The roll-damping moment coefficient, on the other hand, is much more difficult to measure and requires a free spinning rig in association with a sting balance. The damping moment can also be deduced from the free-flight motion in an instrumented firing range by recording the projectile spin history using a marking point (usually a base pin) and data reduction of spark shadowgraph film plates. Therefore, a method to adequately estimate the roll-damping moment coefficient, C_{lp} , is needed.

Eastman¹ observed the algebraic relation provided by Bolz and Nicolidas² and applied the theoretical expression of Adams and Dugan³ only to find that it did not fit the array of configurations to which it was applied. Eastman then empirically established his correlation and showed that it well fitted the experimental data. Eastman's correlation was declared valid only for bodies with four fins in cruciform (i.e., "plus", +) formation, basically because it had its roots in the Adams and Dugan analysis. However, the empirical change that Eastman has made should have removed that restriction, except that Eastman never applied the correlation to any fin setting other than the cruciform formation. In recent efforts, a need has risen for estimating the roll damping for curved wraparound fins and for fin sets with three- or six-fin panels. The effect of the curved fin surfaces and the arbitrary number of fins had to be addressed. In addition, it was not known whether the earlier correlation will hold true for offset fins (those mounted at an angle other than 90° with the body circumferential tangent line, as shown in Figure 1).

Analytical and semi-empirical methods^{3, 4, 5, 6} are used in the literature to estimate C_{lp} and/or $C_{l\delta}$. Difficulties arise because of the need to identify the assumptions and limitations of each analysis or empirical method, so one knows in advance if the fin configuration and fin panel number are acceptable. Also very often, only supersonic speed regimes are considered because of the relative ease in using the linearized supersonic theory. Thus, transonic and subsonic applications are seldom studied or covered.

The present extended correlation takes advantage of the more available and usually more accurate values of $C_{l\delta}$ (whether measured or computed) to evaluate the more difficult to measure and usually elusive C_{lp} . The present correlation is applicable to a wider range of configurations than all earlier relations. Application to configurations with six fins indicated the validity of the correlations to non four-panel cruciform fins. Application to fins with offset angles between 45° and 135° also confirmed the validity of the correlation for that fin type. Finally, the effect of fin panel curvature of a three-panel curved wraparound fin configuration is also included in the extended correlation.

An approximate engineering method for estimating $C_{l\delta}$ from fin C_N is presented and proved to be surprisingly more accurate than the more widely used semi-empirical method of Ref. 7.

2. ANALYSIS

To understand and explain the present correlation, one has to discuss its origin and relation to the pure rolling motion equation of symmetric missiles. The analysis and justification of the extended correlation are discussed next.

2.1 The Pure Rolling Motion Equation The equation of rolling motion about the body axis is usually written as

$$(C_{l\delta}\delta + C_{lp}(pd/2V)) \cdot q_{\infty} A_{ref} d = I_x \ddot{\phi} \quad (1)$$

in which the roll-producing moment coefficient C_l attributable to the fin cant angle δ is usually written as the coefficient derivative $C_{l\delta}$ multiplied by the cant angle δ . The opposing moment (damping moment) is usually written as the multiple product of the coefficient derivative, C_{lp} , times $(pd/2v)$. Note that in the present work, as in Ref. 1, C_{lp} is defined as

$$\frac{\partial C_l}{\partial (pd/2V)}$$

with the "2" inserted. Also, $p = \dot{\phi}$ = the roll rate. The reference area, A_{ref} , is always based on the body reference diameter and equals $\pi d^2/4$. The damping (opposing) roll moment derivative coefficient, C_{lp} , has a negative sign as will be observed.

For the steady-state roll motion, $\ddot{\phi}=0$ and therefore,

$$\frac{C_{lp}}{C_{l\delta}} = -2(V\delta/p_s d) \quad (2)$$

Note that if $C_{lp}/C_{l\delta}$ is to be constant (with time) the p_s (the steady state roll rate) must vary identically with the velocity along the trajectory. However, for projectiles (unpowered), the velocity decreases. Thus, p must also decrease to keep the ratio $C_{lp}/C_{l\delta}$ constant. Therefore, if p decreases, then true "steady-state roll" does not exist. Therefore, if the ratio of C_{lp} to $C_{l\delta}$ is constant along the trajectory, then this does not translate to a true steady state spin value and vice versa.

Bolz and Nicolidas found, after their range testing of the basic finner projectile, that the ratio of $C_{lp}/C_{l\delta}$ is invariant with Mach number. However, they also called this ratio erroneously "steady-state fin tip helix angle per cant angle" because their "steady-state" referred to the 600-foot-long range measurement where the velocity of the projectile does not significantly decrease, and thus, the velocity is taken as "constant" at its midrange value.

2.1.1 The Cant Angle and Equivalent Cant Angle Originally, the cant angle, δ , refers to the angle between the body axis and the chord line of the cross section of the whole fin panel, as depicted in Figure 2. The fin panels are "deflected" in one direction for all (or some) fin panels as may be needed. For a cruciform fin setting, one panel will be up and the 180° opposing fin panel will be down, causing an opposite fin normal force to form the rolling moment, l . However, most present-day projectile fins are only "partially" canted,

i.e., the fin cross section chord line is still parallel to the body axis with only the leading or/and trailing edge being chamfered at an angle to the fin chord line. This is usually done for two reasons. First, the whole panel deflection may be producing too much spin which may be undesirable, although a very small whole panel cant may be possible (of order of 0.1°). This last alternative is usually not recommended due to the relatively large errors in the manufacturing accuracy. Second, the manufacturing cost and accuracy are improved for the partial canting which maintains the fin chord aligned with the body axis, while only chamfering the leading and/or the trailing edge. For projectile applications with only partial canting, an equivalent whole fin panel cant angle, δ_{eq} , must be determined and used if $C_{l\delta}$ is to be evaluated from the measured value of C_l .

2.2 The Correlation of Eastman Bolz and Nicolidas published their results in 1950. Adams and Dugan followed in 1958 by publishing their supersonic analysis using the linearized perturbation theory for slender bodies. They extended a two-wing airplane configuration analysis to a four-fin body in the plus (+) formation (i.e., cruciform fins). For the cruciform fins, they obtained the expression

$$\frac{C_{lp}}{C_{l\delta}} = -0.627(d/b_o) \quad (3)$$

in which b_o is the total span of two-fin panels including the center body diameter. Unfortunately, they never applied this result to any configuration or compared it to any data. Eastman applied Adams and Dugan's expression in 1986 to several configurations for which data existed for both C_{lp} and $C_{l\delta}$, to ascertain that their result did not hold true. From these experimental data for C_{lp} and $C_{l\delta}$, Eastman empirically wrote the following correlation in a form similar to the result of the analysis of Adams and Dugan.

$$\frac{C_{lp}}{C_{l\delta}} = -2.15(y_c/d) \quad (4)$$

in which y_c is the distance between the rolling body axis to the area center of one fin panel. Eastman showed that his correlation was valid not only for supersonic speeds as Adams and Dugan's analysis implied, but rather for all speed regimes. Eastman, however, wrongly limited his correlation to four cruciform fin configurations, since he thought mistakenly that the changes he made in Adams and Dugan's expression were minor, and therefore, the limitations of their analysis must be implied to it. Eastman never applied the correlation to noncruciform fins or to an arbitrary number of fins (i.e., other than four fins). Following, this exact issue is addressed in detail.

2.3 Extension to an Arbitrary Number of Fins Eastman's empirical correlation, Equation (4), does not come close in the numerical value to that of Adams and Dugan's of Equation (3). Although Eastman had started with Adams and Dugan's expression, he ended with an expression, that was similar in form, but is unrelated to the outcome of their analysis. Therefore, Eastman's expression should not be restricted to Adams and Dugan's limitations of being derived for four cruciform fins only. Equation (4) is purely empirical and does not come as the output of the Adams and Dugan analysis. Having establishing this fact, one main task remained: to investigate how well the data would fit the new prescribed correlation

of Equation (4) for fin numbers other than four. In the present work two configurations were considered: one with six fins and another with three fins. Both cases had the correlation of Equation (4) verified satisfactorily. These results are discussed in Section III.

2.4 Extension to Curved, Canted Wraparound Fins Projectiles with curved wraparound fins and no cant angles are known to suffer a reversal in roll direction in the Mach range between 1.0 and 2.0. Although this behavior is not completely understood, it is generally believed to be attributable to the effect of the fins' leading edge shock intersection and their impingement on the rear fin surface, or just altering the flow field between the fins in a manner to produce rolling moment in an opposite direction. In addition, with no intentional cant angle, fin manufacturing tolerances (of order of $\pm 0.05^\circ$) can also have an influencing factor. Uncanted wraparound fins may have C_l values between +0.05 and -0.05. The present analysis only considers canted wraparound fins (i.e., which have actual and intentional cant angles), in which there is no reversal in roll direction. When the curved wraparound fin is analyzed, the fin roll resisting moment is expected to be larger than a similar flat fin with the same fin projected area. However, the roll-producing moment may not increase from the corresponding flat fin panel. If a correlation similar to Equation (4) exists for this case, C_{lp} must be reduced by a factor relating to the curvature of the fin panel. Also this factor must degenerate to the value of 1.0 for the correlation to be valid for noncurved fins as well. The form for the C_{lp} reducing factor was chosen as $(l/h)^m$ in which m is an exponent that varies with Mach number to reflect the fin leading edge shock intersection effects, (l/h) is the ratio of the arc length of the curved fin chord to the distance between the two fin end points, as shown in Fig. 1. The exponent m was found to vary with M as $0.1[1 + M + (2/3)M^2]$, based on the experimental data of C_{lp} and C_{ls} of Ref. 10.

Thus, the new extended correlation is therefore written as

$$\frac{C_{lp}}{C_{ls} \cdot (y_c/d) \cdot (l/h)^m} = -2.15 \quad (5)$$

Note that for flat fins, $(l/d)^m$ is equal to 1.0 and the new correlation degenerates to the form of Equation (4). The applied case of Ref. 10 is discussed in Section III. Recently, numerical computations were made¹¹ to compute C_l for uncanted wraparound fins.

2.5 Extension to Projectiles With Offset Fins Renewed interest has surfaced regarding configurations with offset fins. Offset fins are those erected at an angle B to the tangent to the missile body cross section, as depicted in Fig. 1.

One would expect that the rolling moments for offset fins with B greater than 60° would not be greatly less than that of the usual 90° case. However, one also expects that for B less than 45° a large decrease in both C_{ls} and C_{lp} would occur. One question remained regarding whether both C_{lp} and C_{ls} will vary with B in a manner so that their ratio, as prescribed by the general correlation of Eq. (5), is to remain constant.

Recent range firing data for the Ballistic Research Laboratory (BRL) Research Projectile was reported by Kayser¹². Both C_{lp} and C_{ls} were measured for rectangular fins at offset angles of 45° and 90° . The results of the application are given in Section III.

2.6 Fast Evaluation of $C_{l\delta}$ It is obvious from Eq. (5) that to determine $C_{l\delta}$, one needs to have the value of $C_{l\delta}$ available. Several analytical³, semi-empirical⁷, and computer codes^{7,8} are available in the literature to estimate it. None of these methods is direct, accurate, or valid for all speed regimes. Each method has its limitations and regime of validity. It is difficult from the written documents of each method to identify exactly all the assumptions or the empiricism involved.

A suggested simple method that will suffice for most cases is therefore presented here. It is based on the more readily known normal force slope coefficient, $C_{N\alpha}$, for the fins. This coefficient is usually more available and readily computed routinely from fast aerodynamics prediction codes such as those of Refs. 7 and 8. This coefficient is computed with no spin effect included. In the present work, the code of Ref. 7 was used to estimate C_N from $C_{N\alpha}$.

As shown in Figure 3, for a cruciform fin at an angle of attack α but at no cant (deflection) angle δ , only fin panels No. 2 and 4 will produce normal force as presented by C_{NF2} and C_{NF4} . Therefore, from the total non-spinning body computations of the code of Ref. 7, the fin normal force (including both the body-fin and fin-body interferences) is computed by subtracting the body-alone normal force from the total configuration normal force.

$$C_{NF2} = C_{NF4} = (C_{Ntotal\ config} - C_{Nbody-alone})/2. \quad (6)$$

The factor of 2 in the above equation reflects a one fin-panel contribution in a four-panel fin configuration, as computed using the code of Ref. 7. Now, considering the spinning case, with no angle of attack α but with the four fin panels wholly deflected by an angle δ ($\delta = \alpha$), one can easily compute the roll-producing moment C_l as

$$C_l = (n \cdot C_{NF2} \cdot y_c)/d \quad (7)$$

in which n is the number of canted fins in a set of N fins, y_c is the arm of the fin panel normal force about the body axis, measured to the fin area geometric center. The d in Eq. (7) is for the reference length in the definition of C_l . Once C_l is computed, the $C_{l\delta}$ is simply computed as C_l/δ , assuming small δ of less than 10° .

The only approximation in Eq. (7) is the use of y_c , which refers to the fin area center rather than the fin pressure center, as it should theoretically be. However, the fin semi-span is usually of order of one body diameter, and therefore, the difference between the area and pressure centers is quite small (of the order of about 5%).

One major advantage of using Eq. (7), is the inclusion of the effect of the fin-body and body-fin interference effects through the computed C_{NF2} . This effect is considerably larger (can be 30% of the fin-alone normal force) and is implicitly included by using the code of Ref. 7. Other methods^{4,5,6} are less accurate because of either failure to include these effects or because the estimates of their values were inadequate, if they were included. The error in using y_c , instead of y_{cp} , results in much smaller effect than neglecting or miscalculating these interference effects. An example of application of this present approach to the basic finner projectile and comparison to other methods for calculating $C_{l\delta}$, is given in Section III.

3. RESULTS OF APPLICATION TO DIFFERENT CONFIGURATIONS

Following are the results of applying the extended correlation of Eq. (5) to seven different configurations. These seven cases include four cases applied in Ref. 1; however, details of the fins are provided herein together with all the tabulated experimental data to provide a complete archival data for future use and verification.

3.1 The M829 Kinetic Energy Projectile (Arbitrary Number of Fins) This is a subcaliber, sabot projectile fired from a 120-mm smoothbore gun. It is launched at a speed of 5800 ft/s (1767.7 m/s). The configuration has six fins and a reference diameter of 27-mm (1.065 inch) and is depicted in Figure 4.

Range data were collected for 11 shots fired. The value of an equivalent angle, δ_{eq} , for a whole panel was estimated⁹, based on detailed fin drawings, to be 0.55° . The range data and the present prediction for C_{lp} are provided in Table 1. The listed C_{lp} range values were divided by 2 to conform to the (pd/2V) notation. In Figure 4, the C_{lp} values computed by the correlation at the same Mach number were averaged to provide a single value. The individual values, however, are provided in Table 1. Figure 4 indicates that for a six-fin configuration, the correlation proved to be valid without any adjustment. Therefore, Eastman's limitation to only four cruciform fins is not justified and is therefore removed.

Table 1. Data and Results for the M829 Projectile

<i>MachNumber</i>	<i>C_{ls}(data)</i>	<i>C_{lp}(data)</i>	<i>C_{lp}(Eq.(5))</i>
3.50	9.85	-18.04	-20.44
3.53	16.35	-32.28	-33.90
3.57	8.23	-16.14	-17.06
3.98	11.49	-22.68	-23.83
4.02	11.48	-19.46	-23.80
4.64	10.83	-25.30	-22.47
4.64	8.61	-19.26	-17.86
4.67	10.19	-21.92	-21.13
5.25	11.34	-20.38	-23.52
5.26	8.80	-17.40	-18.25
5.27	9.30	-21.72	-19.29

3.2 The HYDRA 70-mm MK66 Army Missile (Curved Wraparound and Arbitrary Number of Fins) The U.S. Army 70-mm (2.75-inch) HYDRA MK66 missile is shown in Figure 5. It has three wraparound fins with partial fin cant. The main body with its rocket motor can carry different warhead configurations. A combination of wind tunnel and flight testing was made¹⁰ and the data are given in Table 2. This case was used to

establish the fin curvature modification correction of Eq. (5). Figure 5 gives the comparison for the present correlation constant of 2.15 and that obtained from the original experimental data. The largest deviation is observed in the range between $M=1$ and $M=2$. The agreement gets much better after $M=2$. The Mach number correction model for the leading edge shock intersection effect proved to be adequate. Notice the lack of the fin shock intersection effect in the earlier Eastman's correlation result. This effect led to an error in C_{lp} as high as 30% underprediction at $M=3$, as shown in Fig. 5. Noted is also the application in this case to the three fins rather than the four-fin restriction of Ref.1. Therefore, the present correlation of Eq. 5 has been shown to be valid for an arbitrary number of fins, as was also validated in the previous application to the six fins of the M829 projectile.

Table 2. Data and Results for the HYDRA 70-mm MK66

<i>MachNumber</i>	$C_{ls}(data)$	$C_{lp}(data)$	$C_{lp}(Eq.(5))$
0.0	2.92	-5.60	-5.65
0.6	2.98	-6.10	-5.94
0.9	3.09	-6.40	-6.29
1.0	3.21	-6.90	-6.55
1.1	3.49	-7.80	-7.22
1.15	3.67	-8.05	-7.63
1.3	4.01	-8.15	-8.45
1.6	3.90	-8.00	-8.46
1.9	3.49	-7.60	-7.84
2.2	3.09	-7.10	-7.21
2.5	2.81	-6.70	-6.85
3.0	2.29	-6.00	-6.04

3.3 The BRL Research Projectile (Offset Fins) This projectile is a scaled down model of 40-mm (1.57-inch) diameter and of length to diameter ratio of 10. Its model is shown in Figure 6. It was test fired at BRL (now Army Research Laboratory [ARL]) from a 105-mm rifled gun tube, using a discarding sabot. Three models with different fin shapes were tested. The first was of a quarter-ellipse (approximately) fin planform. The second was of a rectangular form, while the third was a clipped delta (trapezoidal) configuration. All these sets of fins had four fin panels. The clipped delta was tested at both 90° and 45° offset angles. Range firing for 15 projectiles was reported, including cant angles of 2° and 0.2° . Five rounds of the 15 were fired for the 0.2° cant and are excluded from the present study because the values of C_{ls} are very small and undependable, specially when considering the manufacturing accuracy for a 0.2° cant angle, which can be off by 50%. The wiggly result for the C_{lp} of Fig. (6) for the elliptical fins, reflects the use of the corresponding experimental values of C_{ls} in Eq. (5).

The clipped delta fin with 45° offset angle provided only about 70% of the C_{lp} and C_{ls} of the corresponding 90° offset angle case, but the ratio of these two coefficients still validated

the present correlation of Eq. (5) without any required change as also shown in Fig. 6.

Thus, it is concluded that for offset fins greater than or equal 45° (up to 135°), the present correlation is valid. The tabulated results are given in Table 3. Notice that the range data for C_{lp} were divided by 2 to conform to the $(pd/2V)$ definition.

Table 3. Data and Results for the BRL Research Projectile

<i>Mach</i> <i>Number</i>	<i>FinPlanform/</i> <i>Offset Angle</i>	$C_{l\delta}$ (data)	C_{lp} (data)	C_{lp} <i>EQ.(5)</i>
1.632	<i>Clip.Delta</i> – 45°	2.35	– 3.14	–33.38
1.683	<i>Clip.Delta</i> – 90°	3.15	– 4.74	– 5.01
1.633	<i>Rectangular</i>	10.64	–10.66	–10.61
2.227	"	3.57	– 6.22	– 6.72
0.934	<i>Elliptical</i>	3.57	– 5.54	– 5.83
1.134	"	2.97	– 4.96	– 4.85
1.370	"	3.49	– 5.80	– 5.70
1.643	"	3.31	– 5.46	– 5.41
1.899	"	3.77	– 5.98	– 6.16
2.241	"	4.07	– 6.34	– 6.62

The following cases, number 4 through 7, are presented to confirm the exact data and configurations that the earlier work of Ref. 1 had reported. It is noted that the present correlation of Eq. (5) will degenerate to Eastman's form for any flat fin ($l/h = 1.0$), for any Mach number.

3.4 The Terrier-Recruit First-Stage Vehicle This is an 18-inch (457.2-mm) diameter vehicle with about 27.5 ft length (90.23 m), as depicted in Figure 7. It has four simple flat fin panels. Wind tunnel tests were performed and reported in Ref. 12. Data are given for speeds between $M=0.1$ and $M=5.0$. The correlation providing the value of 2.15 was extremely accurate for this case, as shown in Fig. 7. The predicted C_{lp} also is extremely accurate compared to the measured values. The tabulated form of the results are given in Table 4. Note that both $C_{l\delta}$ and C_{lp} of the data were adjusted for the reference length to be based on the diameter, rather than the total length of the vehicle, as was given in Ref. 13.

Table 4. Data and Results for the Terrier-Recruit First-Stage Vehicle

<i>MachNumber</i>	$C_{l\delta}(\text{data})$	$C_{lp}(\text{data})$	$C_{lp}(\text{Eq.(5)})$
0.1	14.88	-44.84	-45.02
0.5	16.03	-48.19	-48.49
0.8	17.60	-53.21	-53.23
1.0	19.39	-58.57	-58.64
1.16	21.17	-63.92	-64.03
1.5	19.70	-59.57	-59.59
1.8	16.03	-49.19	-48.49
2.4	10.79	-32.46	-32.67
3.5	8.38	-25.43	-25.36
4.0	7.75	-23.42	-23.45
4.5	5.75	-17.40	-17.42
5.0	4.19	-12.72	-12.68

3.5 The GSRS Boeing Rocket This Boeing modified general support rocket system (GSRS) is shown in Fig. 8. It has a 230-mm (9-inch) diameter and four rectangular flat fins, all of which are wholly canted at 0.95° for the later version of the rocket described here and in Ref. 14. The body has a 4° boattail for the rocket motor nozzle. Wind tunnel tests results were also reported in the same reference. The experimental data showed some scatter from the extended correlation value of 2.15, as seen in Fig. 8. In particular, the values at $M=0.7$ for the measured C_{lp} seem to be higher than expected and do not conform to the pattern that C_{lp} decreases with the lowering of Mach number in the transonic and high subsonic speed regimes. Note that the data values in Table 5 were adjusted to be referenced to a diameter of 230 mm rather than to 210 mm as in Ref. 14.

Table 5. Data and Results for the GSRS Boeing Rocket

<i>MachNumber</i>	$C_{l\delta}(\text{data})$	$C_{lp}(\text{data})$	$C_{lp}(\text{Eq.(5)})$
0.7	1.99	-3.70	-3.16
0.9	2.26	-3.52	-3.60
1.2	1.68	-2.85	-2.67
1.3	1.95	-3.13	-3.10
1.5	2.49	-3.67	-3.97
2.0	2.53	-3.85	-4.03
3.0	1.95	-2.99	-3.10

3.6 The Air Force 2.75-Inch (70m-m) Folding Fin Rocket This 2.75-inch (70-mm) diameter rocket has four folding fins that deploy after firing. Figure 9 provides the general configuration. The fins are deployed with a 45° angle to the body axis. The fins are partially canted only at the tip to produce a roll. A later version (not studied here) included a fin tip bent of 20° to produce the same roll. Wind tunnel data are given in Ref. 15. The numerical results of the tests are given in Table 6. The $C_{l\delta}$ values were adjusted to be per radian rather per degree as was given in Ref. 15. The correlation for the value of 2.15 seems adequate and the predicted C_{lp} values agree well with the data. The results are shown in Fig. 9.

Table 6. Data and Results for the AF 2.75-inch Rocket

<i>MachNumber</i>	$C_{l\delta}(data)$	$C_{lp}(data)$	$C_{lp}(Eq.(5))$
2.5	11.91	-34.2	-33.11
3.0	9.97	-27.0	-27.70
3.5	7.73	-22.5	-21.49
4.0	6.59	-19.0	-18.31

3.7 The Basic Finner Configuration The early and familiar configuration of the 1950's was flight-tested at the former Ballistic Research Laboratory range in about 1948-49. It was a configuration approved by the U.S. Army, Navy, and the Air Force Services at that time and is shown in Fig. 10. The range results are reported in Ref. 2. The configuration is a 10-caliber-long body with four flat simple fins. For this particular test, the diameter was 0.785 inch (20 mm), with a sharp cone nose of 20° . Also, for this particular test, only two fins of the four panels were canted. Seven models with different cant angles (2° and 4°) were tested and reported. The data given in Ref. 2 were per "one" fin. Table 7 provides the data after adjusting the reference area and reference length to a standard body reference area and diameter, respectively, rather than the fin area and the fin span (including the body diameter), respectively, as was given in Ref. 2. Figure 10 shows the correlation constant, 2.15, to be very accurate. Also, the computed C_{lp} using Eq. 5 provides very good values when compared with the data.

A comparison for the C_{lp} obtained by different methods was made for the basic finner case. First, C_{lp} was directly computed from the NSWC-AP code ⁷. Second, It was computed using the correlation of Eq. 5, with $C_{l\delta}$ being used from the experimental range data. Third, C_{lp} was computed from Eq. 5, using $C_{l\delta}$ as computed from the fast approximate method presented in Section II. The comparison is made in Fig. 11, where the second method provided the best comparison with the experimental C_{lp} data. However, the first method using the NSWC-AP code proved less accurate than the method using the present simple evaluation scheme for $C_{l\delta}$. This result shows that the present method for calculation $C_{l\delta}$ is quite adequate and reasonably accurate when compared to the semi-empirical methods or even

the theoretical methods.

Table 7. Data And Results for the Basic Finner Projectile

<i>MachNumber</i>	$C_{l\delta}(data)$	$C_{lp}(data)$	$C_{lp}(Eq.(5))$
1.59	11.98	-25.04	-24.60
1.64	12.26	-25.86	-25.17
1.69	12.32	-25.63	-25.29
1.75	11.89	-25.03	-24.41
2.25	9.44	-19.54	-19.38
2.42	9.46	-19.44	-19.42
2.68	8.71	-18.39	-17.88

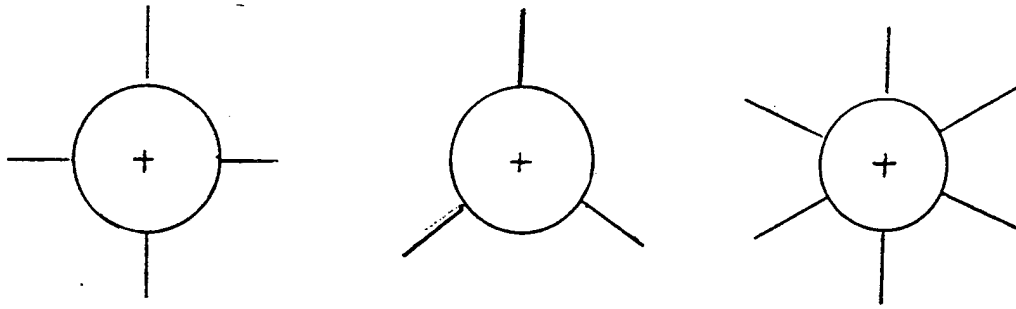
Finally, a compilation of all the cases considered, together with their experimental data, is given in Fig. 12 in comparison with the present extended correlation of Eq. 5. The compilation indicates excellent correlation.

4. SUMMARY AND CONCLUSIONS

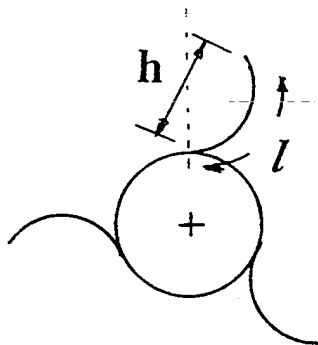
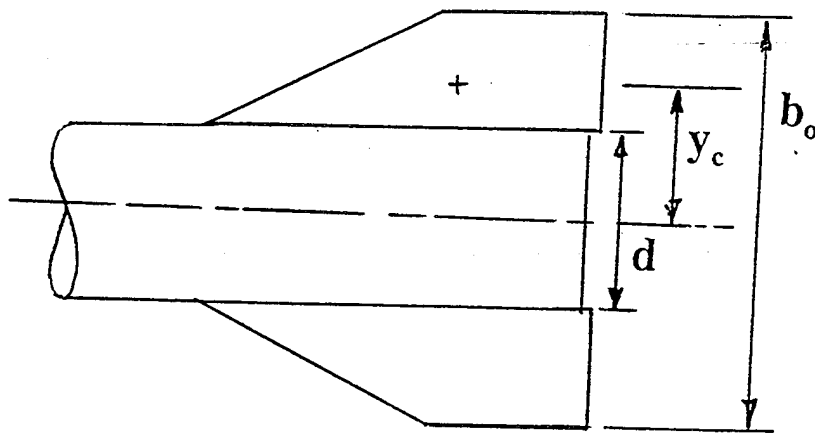
An earlier algebraic correlation is extended to accept more finned missile/projectile configurations. The correlation relates the roll-damping moment coefficient derivative to the roll-producing moment coefficient derivative of the vehicle being studied. The correlation was extended to accept 1) arbitrary number of fins, 2) curved wraparound canted fins, and 3) configurations with offset fins. The correlation extension was based on and verified through experimental data of several different configurations. The correlation was found to be valid over the three speed regimes: subsonic, transonic, and supersonic. The correlation is meant to be used to evaluate the more difficult C_{lp} coefficient, given or knowing $C_{l\delta}$. A simple method to evaluate $C_{l\delta}$ is presented, using the more easier and available C_N coefficient. This method proved to be even better than the lengthy semi-empirical methods used in some fast aerodynamic prediction codes.

This surprisingly simple and apparently universal correlation reduces the number of costly full flow field computations for such complex fin arrangements, if only C_{lp} is sought. It is suggested that new experimental data be applied further to the correlation to still widen its application to any other case which has not yet been considered.

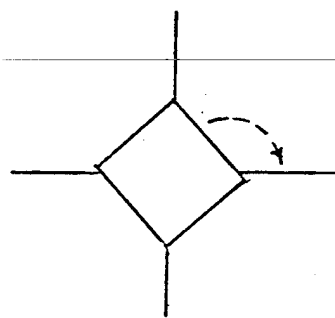
ARBITRARY FIN NUMBER



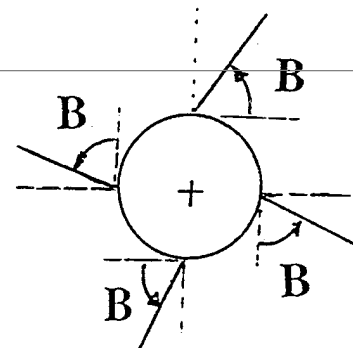
CRUCIFORM (+) FINS



CURVED



FLAT



OFFSET FINS

WRAPAROUND FINS

Figure 1. Nomenclature for fin arrangements.

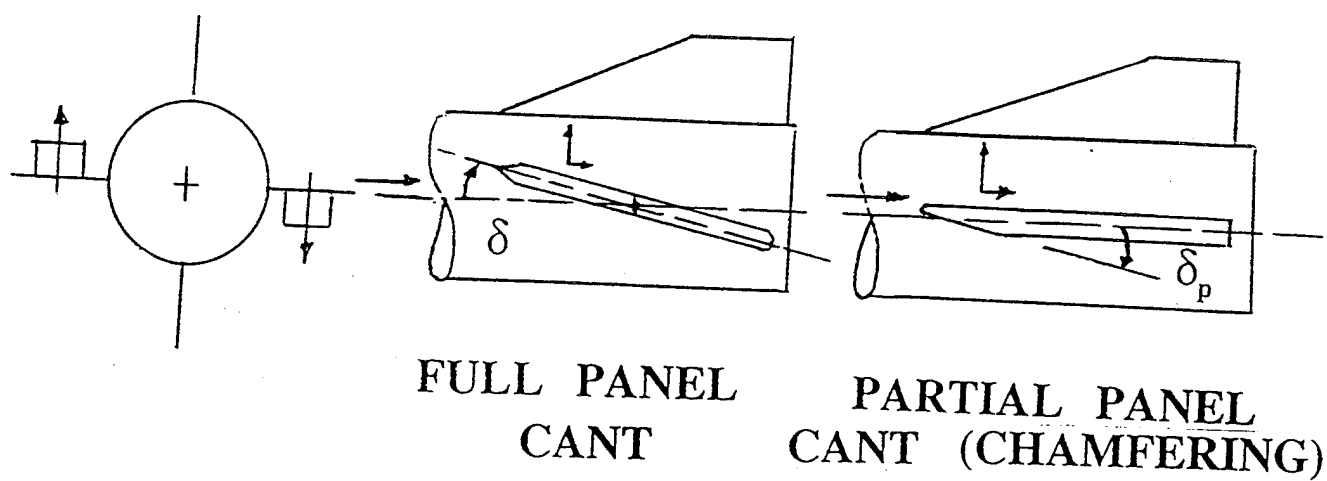
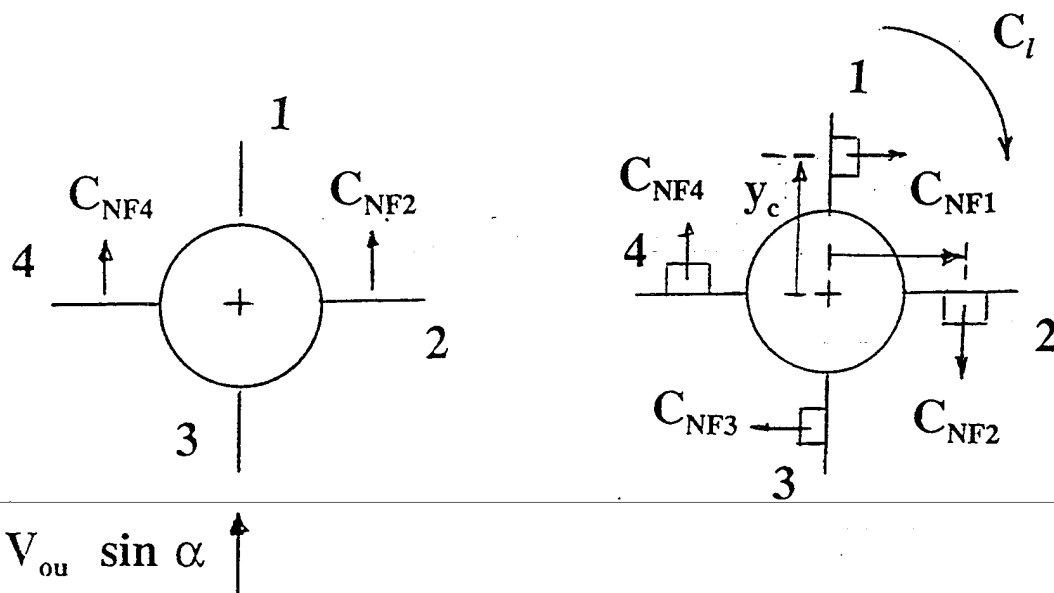


Figure 2. Fin cant (deflection) angle, δ .



Four Fins with No Cant

Four Fins with Cant
Angle δ (δ replacing α)

Figure 3. Nomenclature for estimating C_{l6} from C_N .

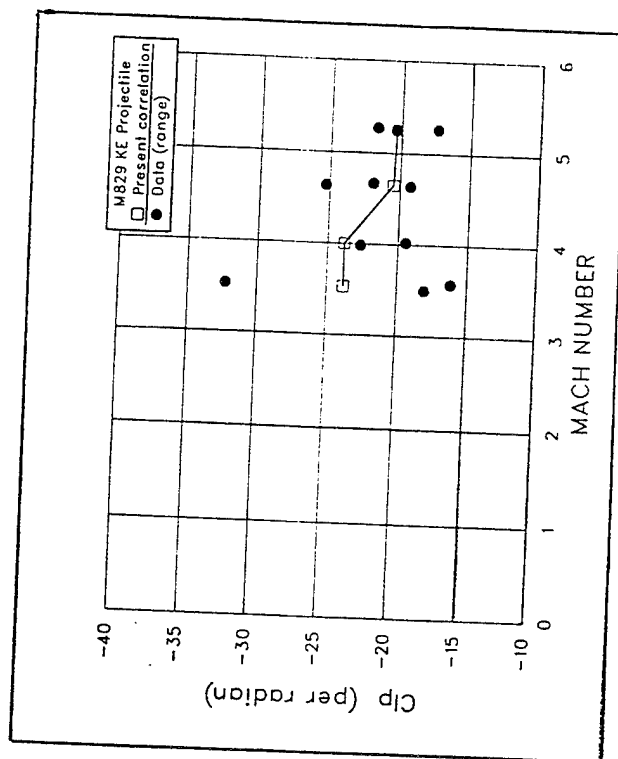
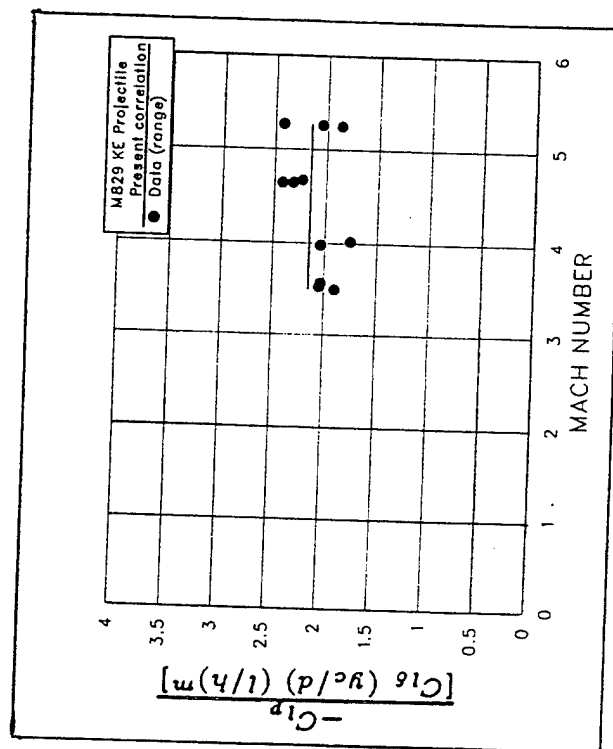
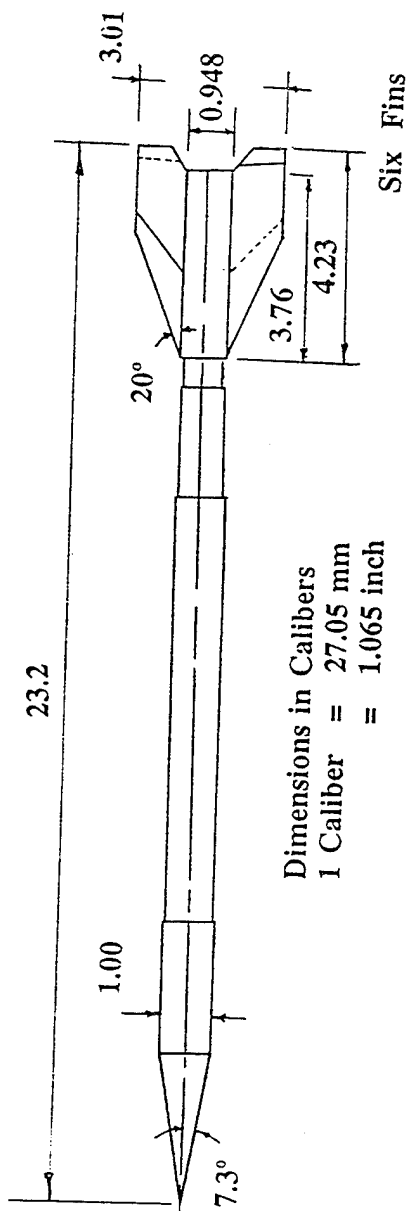


Figure 4. Geometry, validation, and application to the M829 kinetic energy projectile.

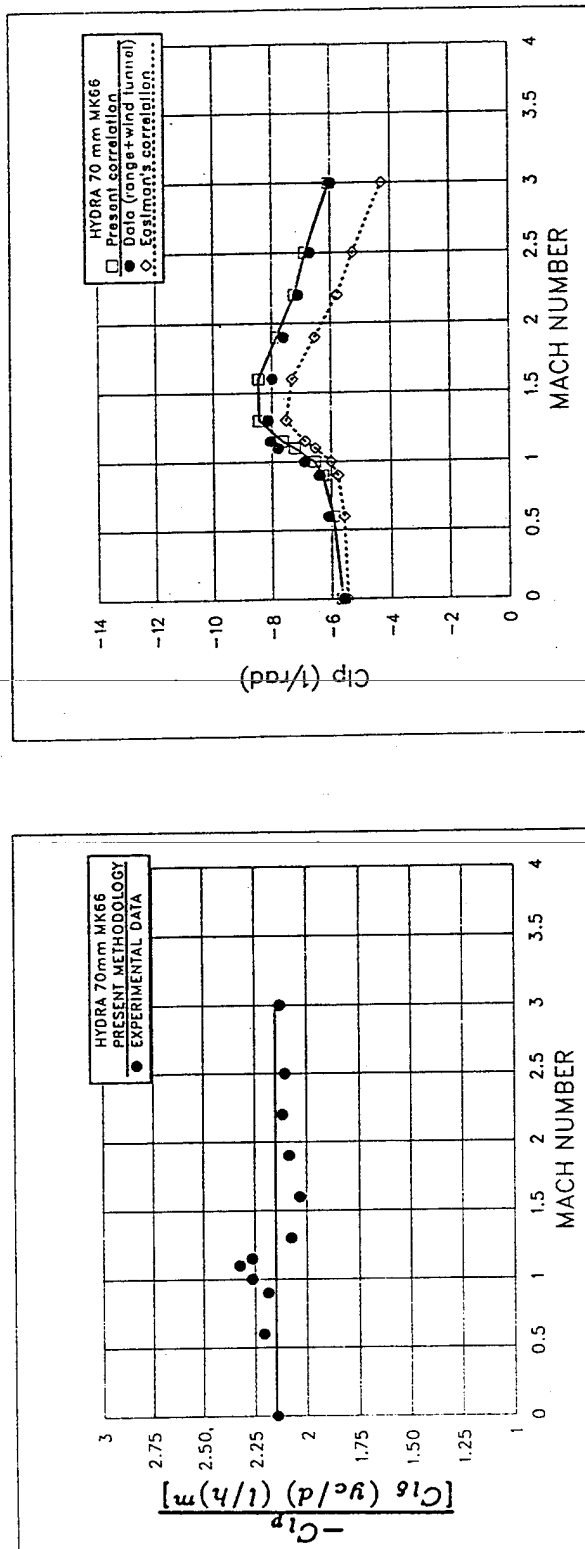
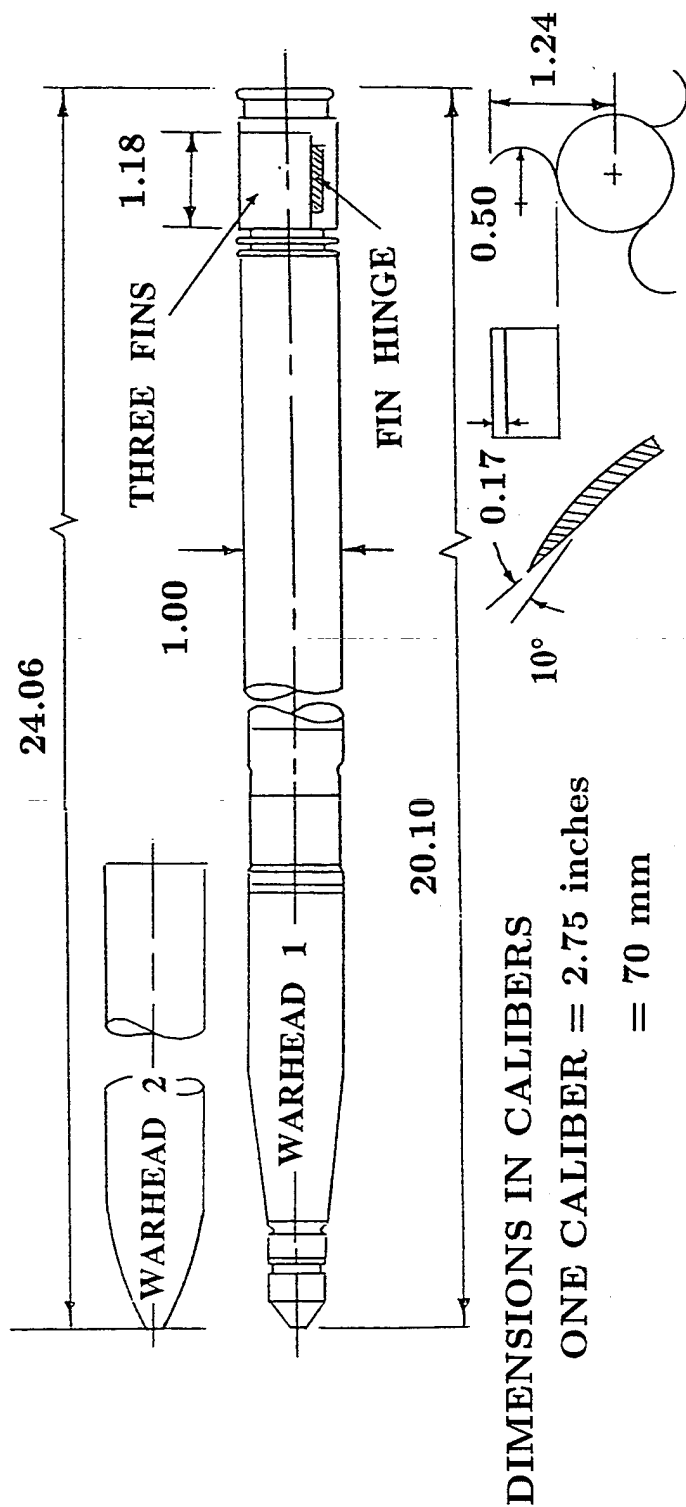


Figure 5. Geometry, validation, and application to the HYDRA 70-mm MK66 missile.

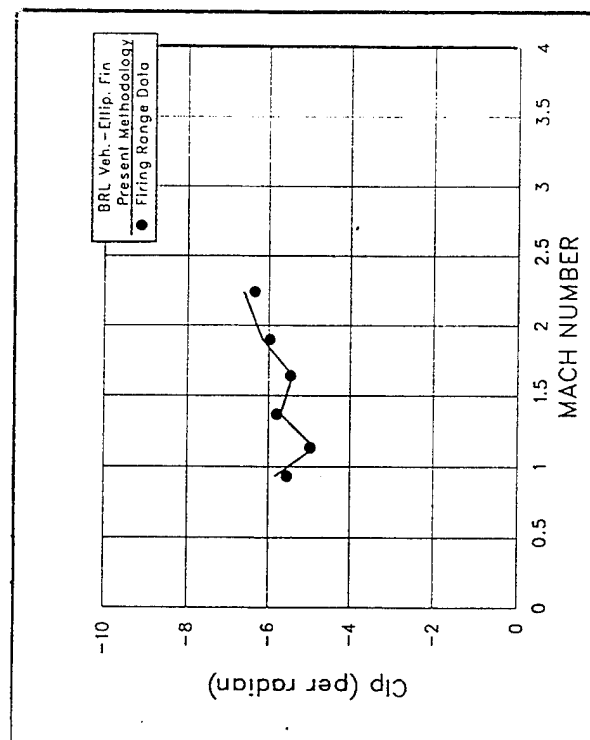
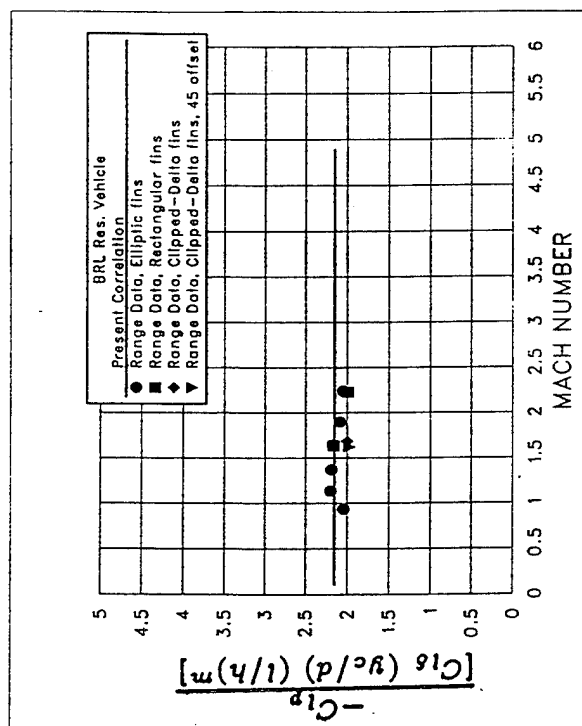
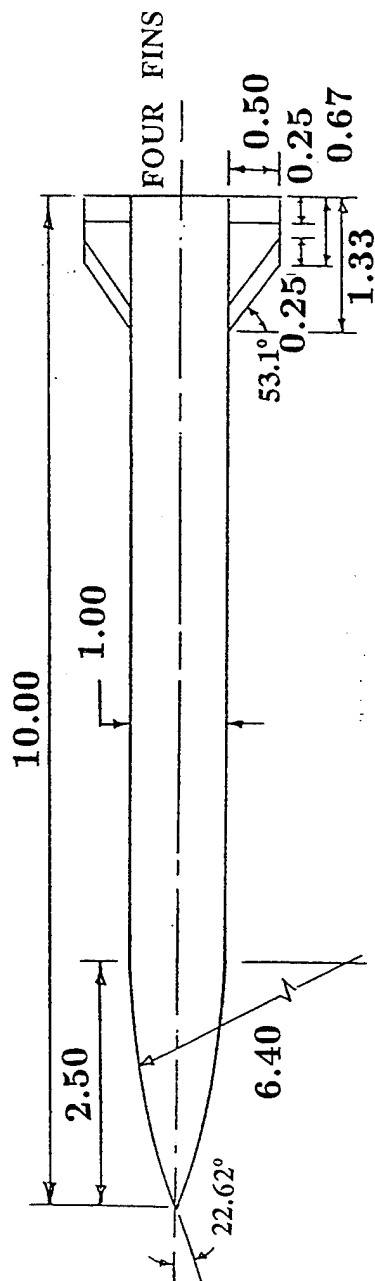
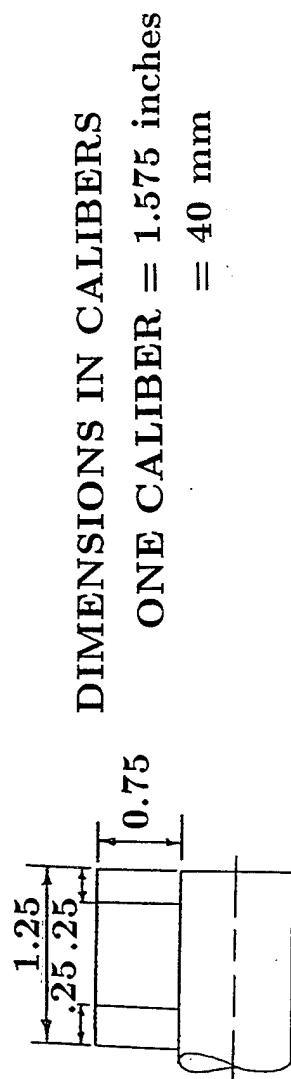


Figure 6. Geometry, validation, and application to the BRL research projectile.

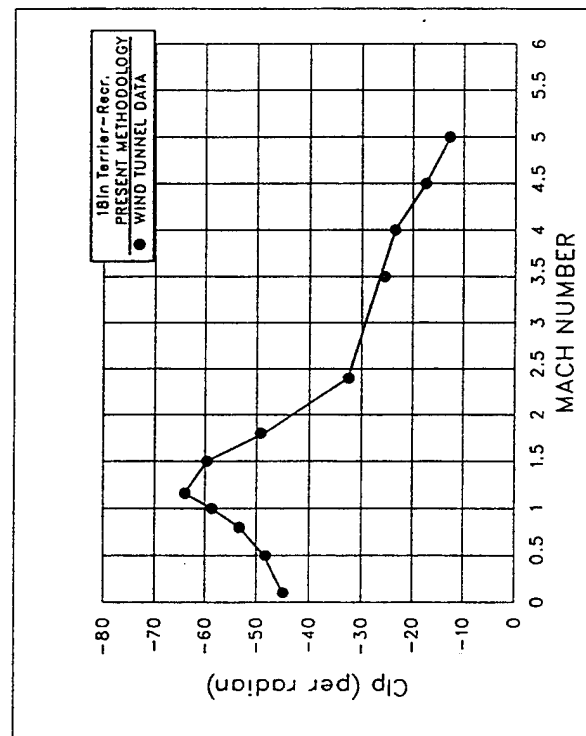
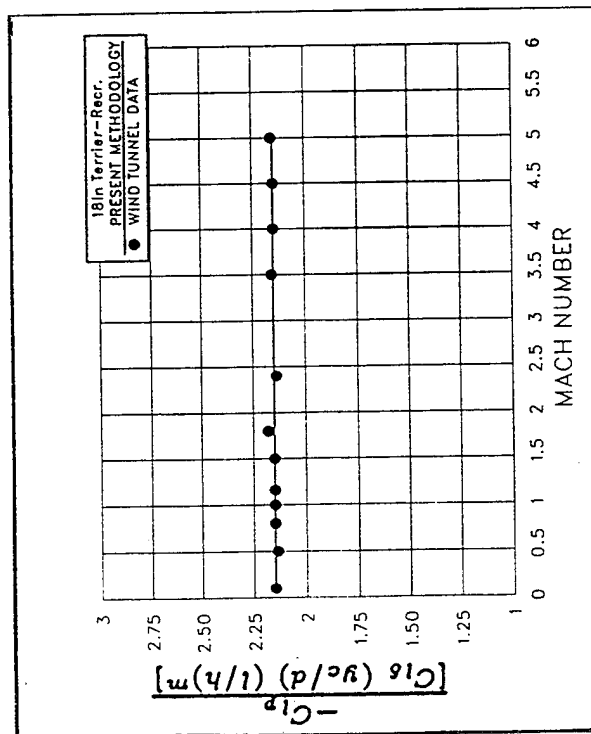
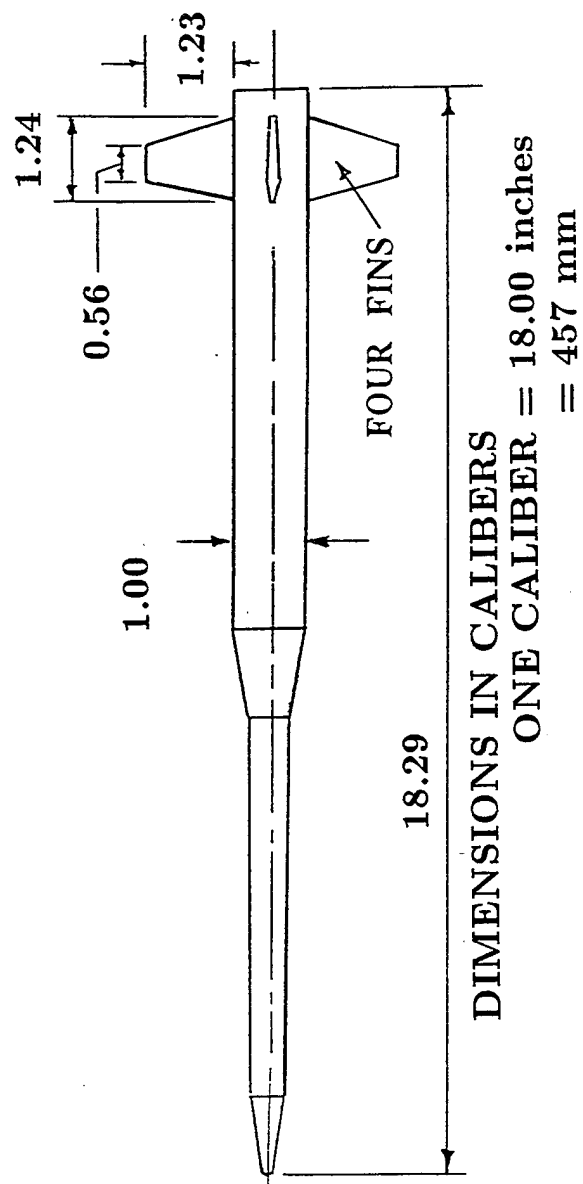


Figure 7. Geometry, validation, and application to the terrier-recruit first-stage vehicle.

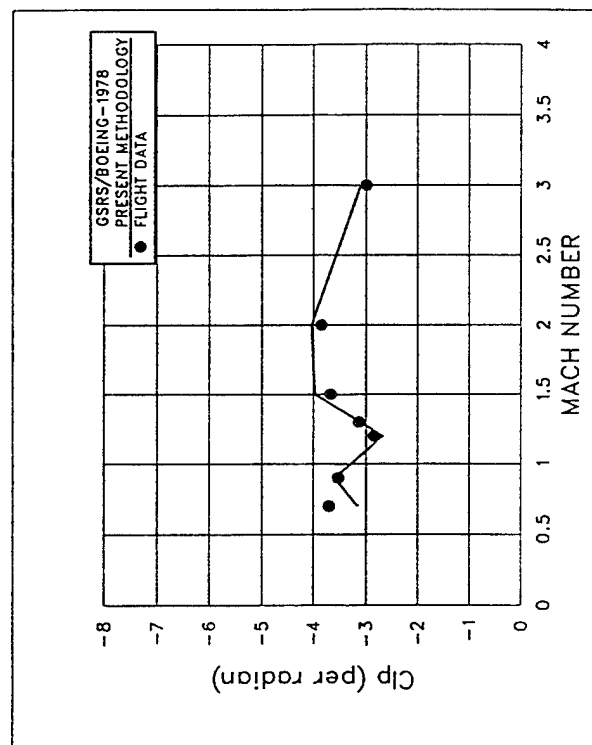
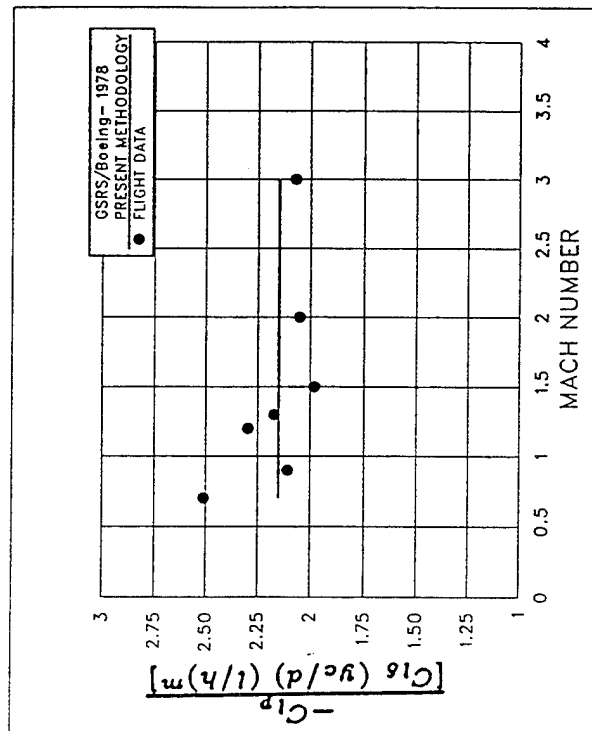
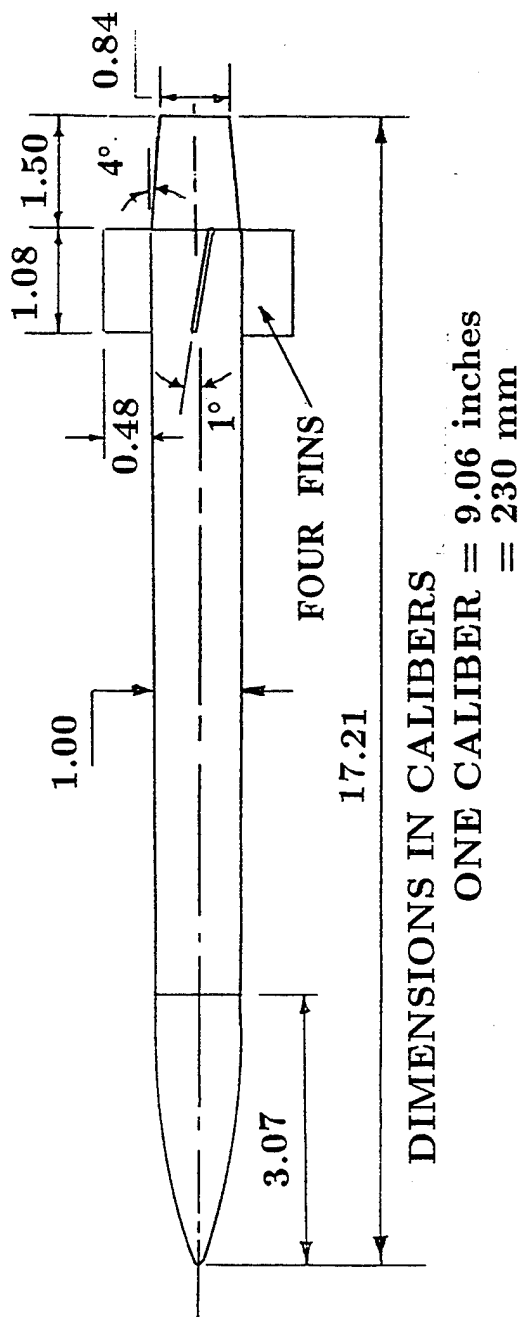


Figure 8. Geometry, validation, and application to Boeing GSRs.

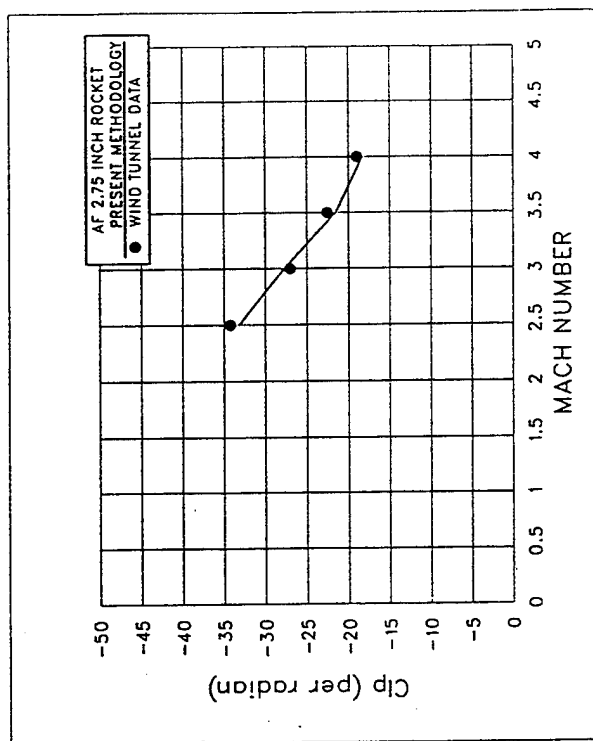
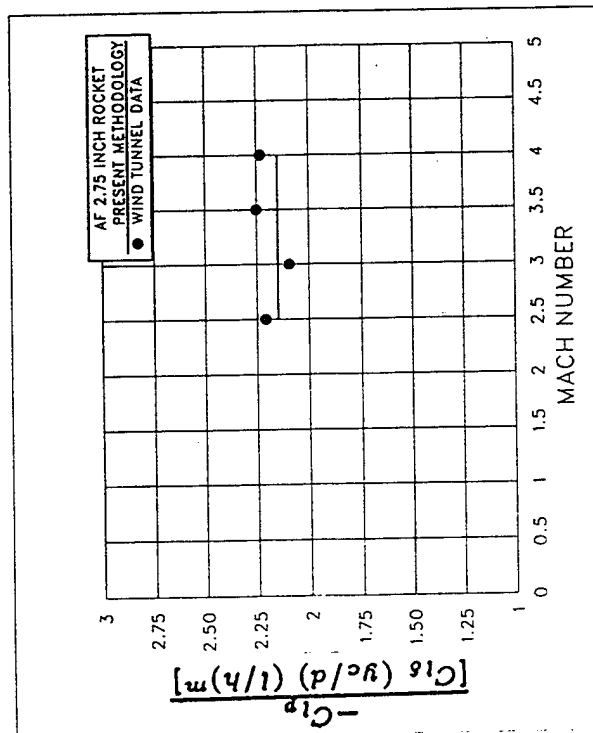
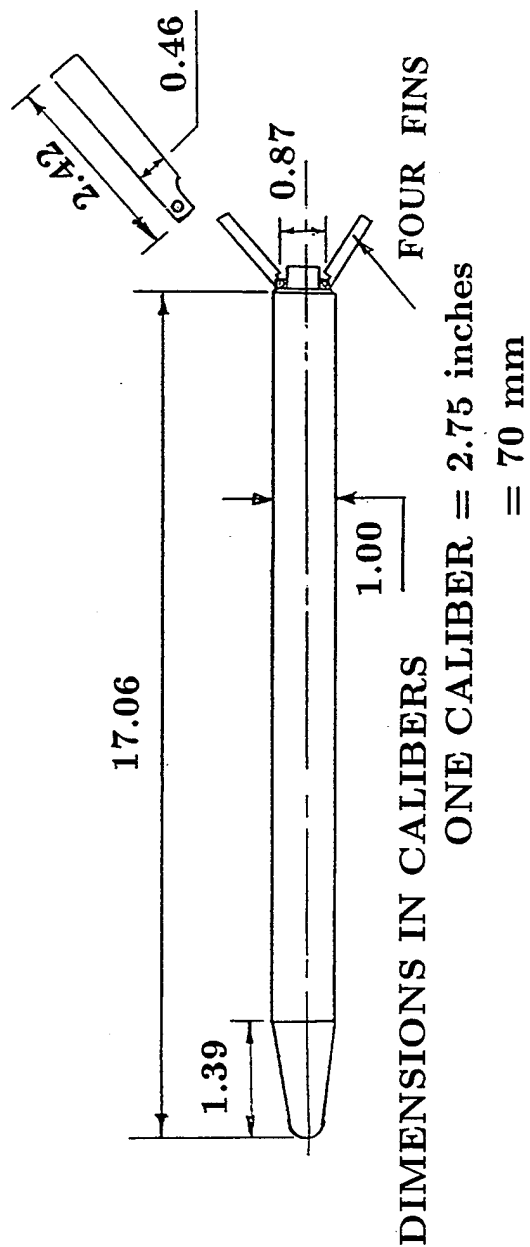
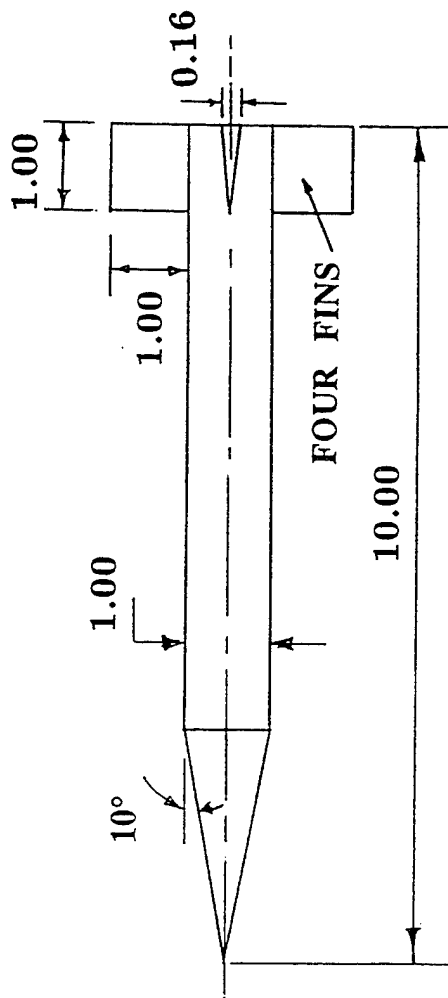


Figure 9. Geometry, validation, and application to the Air Force 2.75-inch (70-mm) rocket.



DIMENSIONS IN CALIBERS

ONE CALIBER = 0.786 inches
= 20 mm

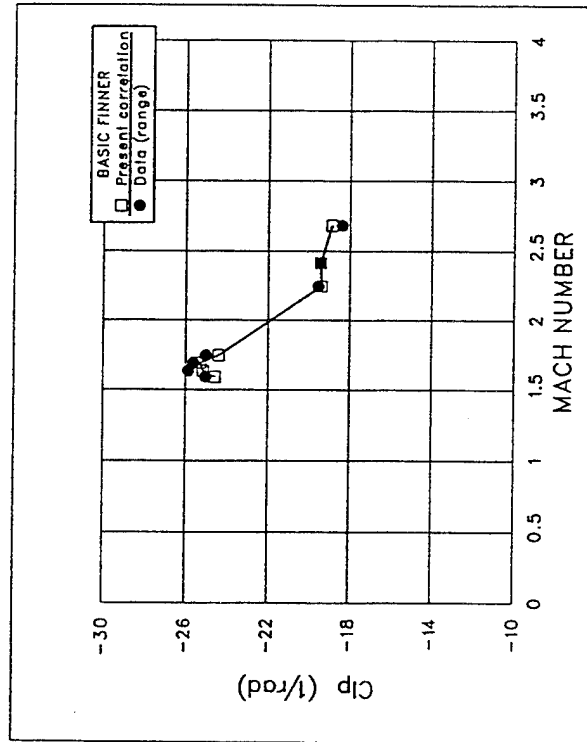
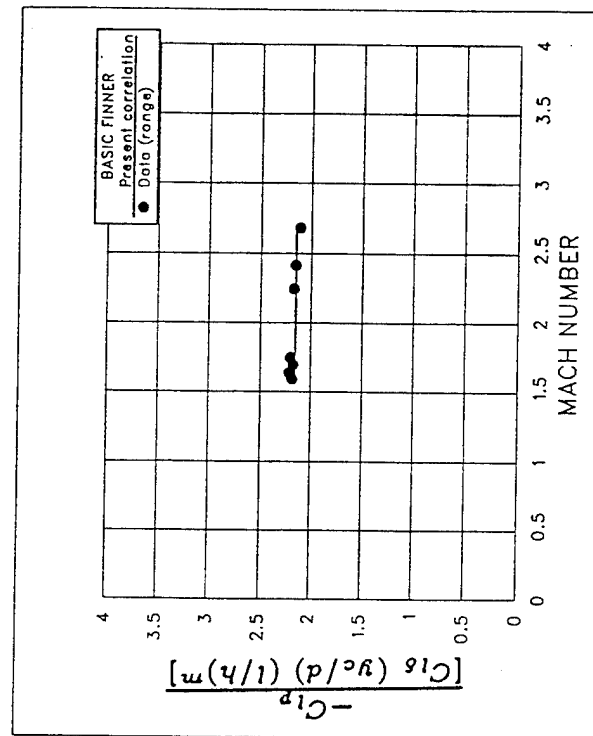


Figure 10. Geometry, validation, and application to the tri-service basic finner projectile.

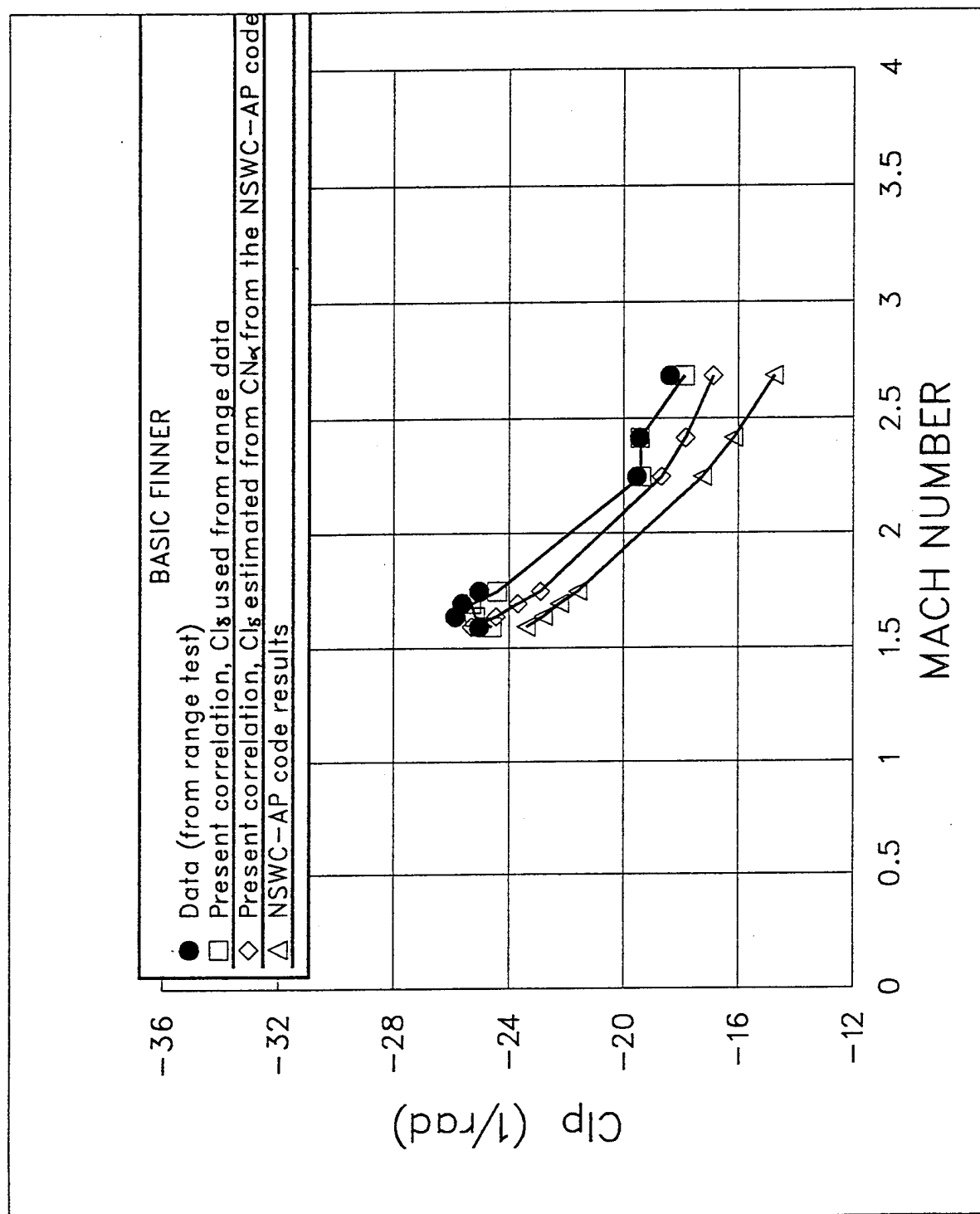


Figure 11. Comparison for C_{lp} computed by different methods.

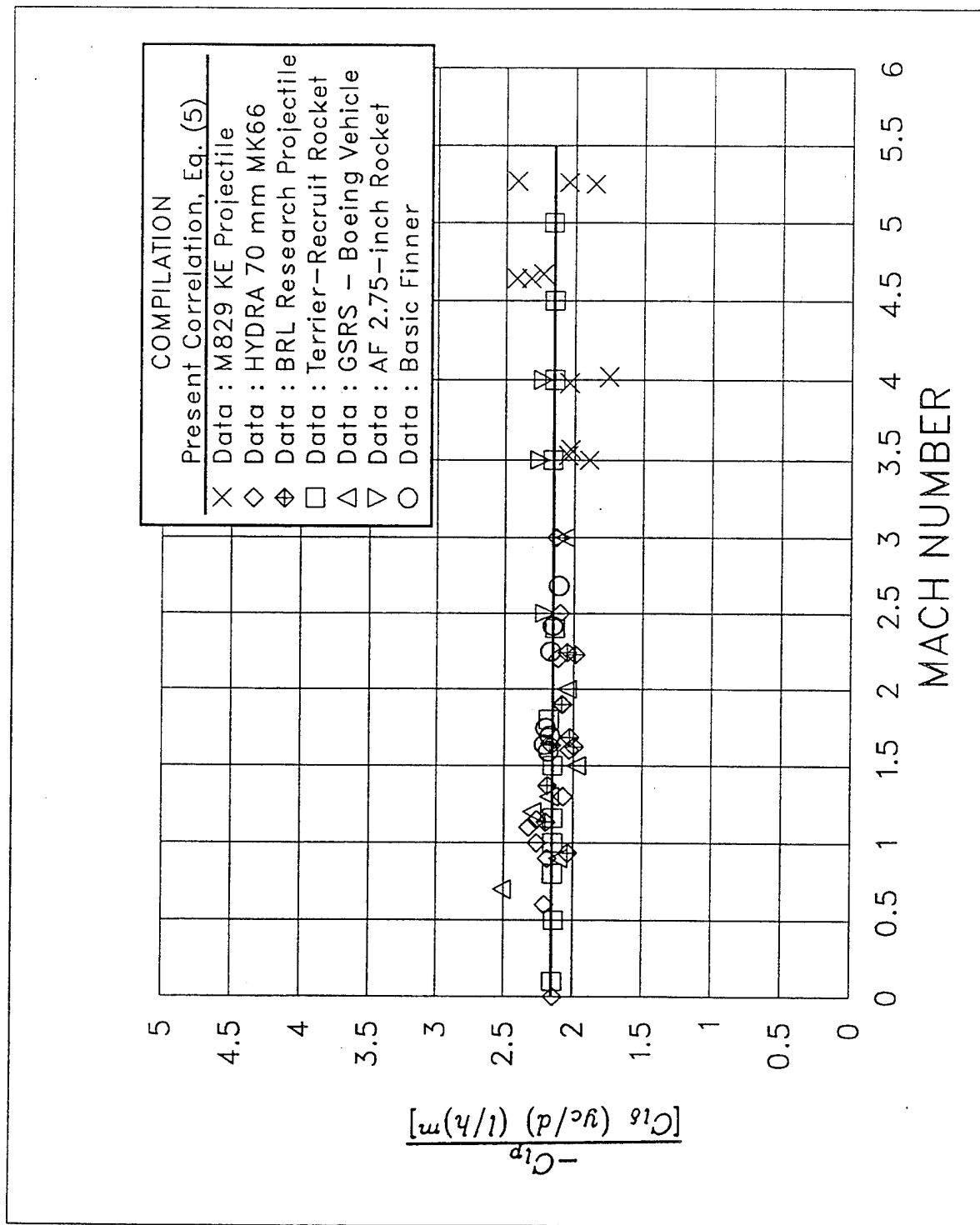


Figure 12. Compilation of all data of all configurations and comparison with present correlation .

5. REFERENCES

1. Eastman, D.W., 'Roll Damping of Cruciform-Tailed Missiles,' Journal of Spacecraft and Rockets , Vol. 23, No. 1, Jan.-Feb. 1986, pp. 119-120.
2. Bolz, R.E. and Nicolidas, J.D., "A Method of Determining Some Aerodynamic Coefficients from Supersonic Free-Flight Tests of A Rolling Missile," Journal of the Aeronautical Sciences, October 1950, pp. 609-621.
3. Adams, G.J. and Dugan, D.W., "Theoretical Damping in Roll and Rolling Moment Due to Differential Wing Incidence for Slender Cruciform Wings and Wing-Body Combination," NACA Report No. 1088, 1958.
4. Barrowman, J.S., Fan, D.N., Obosu, C.B., Vira, N.R., and Yang, R.J. , "An Improved Theoretical Aerodynamic Derivatives Computer Program for Sounding Rockets," AIAA Paper 79-0504, 1979.
5. Oberkampf, W.L., "Theoretical Prediction of Roll Moments on Finned Bodies in Supersonic Flow," AIAA paper No. 77-111, 1977.
6. Prakash, S. and Khurana, D.D., "A Simple estimation procedure of Roll Rate Derivatives for finned Vehicle," Journal of Spacecraft and Rockets, Vol. 21, May-June 1984, PP. 318-320.
7. Devan, L. and Mason, L.A., "Aerodynamics of Tactical Weapons to Mach Number 8 and Angle of Attack 180 : Part II - Computer Program and User's Guide," NSWC TR 81-358, September 1981.
8. Vukelich, S.R., "Automated Missile DATCOM: Vol. I - Program User's Guide," McDonnell-Douglas Corporation Report, St. Louis, MO, August 1984.
9. Weinacht, P. and Sturek, W.B., "Aerodynamics of the Roll Characteristics of the M829 Kinetic Energy Projectile and Comparison With Range Data," BRL-TR-3172, U.S. Army Ballistic Research Laboratory, Aberdeen Proving Ground, Maryland, November 1990. (ADA233175)
10. Dahlke, C.W. and Batiuk, G., "HYDRA 70mm MK66 Aerodynamics and Roll Analysis," U.S. Army Missile Command Report No. RD-SS-90-6, Redstone Arsenal, Alabama, July 1990.

11. Edge, H.L., "Computation of the Roll Moment Coefficient for a Projectile with Wrap-Around Fins," ARL-TR-23, U.S. Army Research Laboratory, Aberdeen Proving Ground, Maryland, December 1992.
12. Kayser, L.D., "Aerodynamics of Fin-Stabilized Projectiles at Moderate Spin Rates," BRL-MR-3965, U.S. Army Ballistic Research Laboratory, Aberdeen Proving Ground, Maryland, April 1992. (ADB163436)
13. Rollstin, L.R., "Aeroballistic Design and Development of the Terrier-Recruit Rocket System with Flight Test Results," Sandia Laboratories Report No. SAND74-0315, Albuquerque, New Mexico, January 1975.
14. Monk, J.R. and Phelps, E.R., "GSRS Aerodynamic Analysis Report," Boeing Company Report, Document No. D328-10055-1, June 1978.
15. Uselton, J.C. and Carman, J.B., "Wind Tunnel Investigation of The Roll Characteristics of the Improved 2.75-Inch-Diameter Folding Fin Aircraft Rocket at Mach Numbers From 2.5 to 4.5," Air Force Arnold Engineering Development Center Report AEDC-TR- 69-207, Arnold Air Force Station, Tennessee, November 1969.

LIST OF SYMBOLS

A_{ref}	= reference area, $(\pi d^2/4)$
B	= fin panel offset angle, degrees
C_D	= drag coefficient, drag force/ $(0.5\rho_\infty V_\infty^2 A_{ref})$
C_l	= rolling moment coefficient, $l/(q_\infty A_{ref} d)$
C_{lp}	= roll moment damping coefficient derivative, $\partial C_l/\partial(pd/2V)$, per radian
$C_{l\delta}$	= roll producing moment coefficient derivative, $\partial C_l/\partial\delta$, per radian
C_N	= normal force coefficient, normal force/ $(q_\infty A_{ref})$
$C_{N\alpha}$	= normal force slope coefficient, $\partial C_N/\partial\alpha$, per radian
C_{NFi}	= normal force coefficient for fin panel no. i
d	= reference diameter
h	= distance between chord end points for curved fin panels
I_x	= axial (polar) moment of inertia about the body geometrical (spin) axis
l	= roll moment, also curved fin chord length
m	= exponent in the new correlation of Equation (5)
M	= Mach number
n	= number of canted panels in a fin set
p	= spin rate of projectile, rad/sec except otherwise noted
p_s	= steady state roll (spin) rate
q	= dynamic pressure, $(0.5\rho V^2)$
V	= projectile velocity
y_c	= radial distance from fin area center to projectile axis

Greek Symbols

α	= angle of attack
δ	= fin cant angle for a whole fin panel
δ_p	= partial fin cant angle (chamfer) at the leading or/and trailing edge of the fin panel
δ_{eq}	= equivalent whole panel fin cant angle for the partially canted (chamfered) fin
ρ	= air density
ϕ	= roll angle, radian
$\dot{\phi}$	= roll (spin) rate, $\partial\phi/\partial t$, rad/sec except otherwise noted
$\ddot{\phi}$	= $\partial\dot{\phi}/\partial t$

Subscripts

∞	= free stream condition
----------	-------------------------

INTENTIONALLY LEFT BLANK.

<u>NO. OF COPIES</u>	<u>ORGANIZATION</u>
2	ADMINISTRATOR ATTN DTIC DDA DEFENSE TECHNICAL INFO CTR CAMERON STATION ALEXANDRIA VA 22304-6145
1	DIRECTOR ATTN AMSRL OP SD TA US ARMY RESEARCH LAB 2800 POWDER MILL RD ADELPHI MD 20783-1145
3	DIRECTOR ATTN AMSRL OP SD TL US ARMY RESEARCH LAB 2800 POWDER MILL RD ADELPHI MD 20783-1145
1	DIRECTOR ATTN AMSRL OP SD TP US ARMY RESEARCH LAB 2800 POWDER MILL RD ADELPHI MD 20783-1145
<u>ABERDEEN PROVING GROUND</u>	
5	DIR USARL ATTN AMSRL OP AP L (305)

<u>NO. OF COPIES</u>	<u>ORGANIZATION</u>
11	<p>COMMANDER ATTN SMCAR AET A C NG J GRAU S KAHN H HUDGINS M AMORUSO E BROWN B WONG W TOLEDO S CHUNG C LIVECCHIA G MALEJKO US ARMY ARDEC PCTNNY ARSNL NJ 07806-5000</p>
3	<p>COMMANDER ATTN SMCAR CCH V B KONARD E FENNELL T LOUZERIO US ARMY ARDEC PCTNNY ARSNL NJ 07806-5000</p>
4	<p>COMMANDER ATTN SMCAR FSE A GRAF D LADD E ANDRICOPOULIS K CHEUNG US ARMY ARDEC PCTNNY ARSNL NJ 07806-5000</p>
6	<p>COMMANDER ATTN SMCAR CCL D F PUZYCKI D CONWAY D DAVIS K HAYES M PINCAY W SCHUPP US ARMY ARDEC PCTNNY ARSNL NJ 07806-5000</p>
1	<p>PROJECT MANAGER ATTN SFAE ASM TMA MAJ B HELD R KOWALSKI TANK MAIN ARMAMENT SYSTEM PCTNNY ARSNL NJ 07806-5000</p>

<u>NO. OF COPIES</u>	<u>ORGANIZATION</u>
2	<p>COMMANDER ATTN STECA EN PM J FALLER D HORTON USA CSTA APG MD 21005</p>
2	<p>COMMANDER ATTN SMCAR DSD T R LIESKE F MIRABELLE US ARMY ARDEC APG MD 21005</p>
3	<p>DIRECTOR ATTN G ANDERSON K CLARK T DOLIGOWSKI US ARMY RESEARCH OFFICE PO BOX 12211 RSRCH TRI PK NC 27709-2211</p>
2	<p>DIRECTOR ATTN AMSRL MA CA M FLETCHER M ODAY US ARMY RESEARCH LABORATORY 405 ARSENAL STREET WATERTOWN MA 02172-0001</p>
2	<p>DIRECTOR ATTN SMCAR CCB R S SOPOK P ALTO US ARMY BENET LABORATORY WATERVLIET NY 12189</p>
3	<p>COMMANDER ATTN CODE DK20 CLARE CODE DK20 MOORE CODE DK20 DEVAN US NAVAL SURFACE WARFARE CENTER DAHLGREN VA 22448-5000</p>
2	<p>COMMANDER ATTN CODE R44 A WARDLAW CODE R44 F PRIOLO US NSWC APPLIED MATH BRANCH WHITE OAK LABORATORY SILVER SPRING MD 20903-5000</p>

NO. OF
COPIES ORGANIZATION

1 DIRECTOR
ATTN MS 258 1 L SCHIFF
NASA AMES RESEARCH CENTER
MOFFETT FIELD CA 94035

2 DIRECTOR
ATTN W OBERKAMPF
W WOLFE
DIVISION 5800 SANDIA NAT LABS
PO BOX 5800
ALBUQUERQUE NM 87185

1 COMMANDER
ATTN AMSMI RD SS AT
W WALKER
US ARMY MISSILE COMMAND
REDSTONE ARSNL AL 35898-5010

2 NASA LANGLEY RSRCH CENTER
ATTN TECH LIBRARY
M HEMSCH
LANGLEY STATION
HAMPTON VA 23665

2 AIR FORCE ARMAMENT LABORATORY
ATNT AFATL FXA
B SIMPSON
G ABATE
R ADELGREN
EGLIN AFB FL 32542-5434

1 LOS ALAMOS NATIONAL LABORATORY
ATTN MS G770
W HOGAN
LOS ALAMOS NM 87545

1 DIRECTOR
ATTN TACTICAL TECHNOLOGY OFFICE
DEF ADV RSRCH PROJ AGENCY
1400 WILSON BOULEVARD
ARLINGTON VA 22209

2 UNITED STATES MILITARY ACADEMY
ATTN M COSTELLO
A DULL
DEPT OF CIV & MECH ENG
WEST POINT NY 10996

NO. OF
COPIES ORGANIZATION

2 SOUTHWEST RESEARCH INSTITUTE
ATTN T JETER
R WHITE
ENERGETICS SYSTEMS
PO BOX 28510
SAN ANTONIO TX 78284

1 BATTELLE NORTHWEST
ATTN M GARNICH
PO BOX 999
RICHLAND WA 99358

2 INSTITUTE FOR ADVANCED TECHNOLOGY
ATTN W REINECKE
D BARNETT
4030 2 W BRAKER LANE
AUSTIN TX 78759-5329

1 AAI CORPORATION
ATTN T STASTNEY
PO BOX 6767
BALTIMORE MD 21204

1 LOCKHEED COMPANY
ATTN J GERKY
PO BOX 33 DEPT 1 330
ONTARIO CA 91761

1 ALLIANT TECHSYSTEMS INC
ATTN MN11 2626
R BECKER
600 SECOND ST NE
HOPKINS MD 55343

NO. OF
COPIES ORGANIZATION

35 DIR USARL
ATTN AMSRL WT, DR I MAY
AMSRL WT P, A HORST
AMSRL WT PB, DR E SCHMIDT
AMSRL WT PD, DR B BURNS
AMSRL WT PA, DR T MINOR
AMSRL-WT-PB,
DR A MIKHAIL (5 CPS)
DR P PLOSTINS
V OSKAY
J GARNER
DR J SAHU
B GUIDOS
P WEINACHT
D SAVICK
H EDGE
DR M BUNDY
DR K FANSLER
DR G COOPER
DR K SOENCKSEN
A ZIELINSKI
DR W DRYSDALE
DR S WILKERSON
AMSRL WT PD (ALC),
A FRYDMAN
T LI
AMSRL WT W,
DR C MURPHY
AMSRL WT WB,
F BRANDON
W DAMICO
AMSRL WT T,
DR W MORRISON
AMSRL WT TC,
R MUDD
R COATES
DR W DEROSSET
AMSRL WT TA,
E RAPACKI

USER EVALUATION SHEET/CHANGE OF ADDRESS

This Laboratory undertakes a continuing effort to improve the quality of the reports it publishes. Your comments/answers to the items/questions below will aid us in our efforts.

1. ARL Report Number ARL-TR-846 Date of Report August 1995
2. Date Report Received _____
3. Does this report satisfy a need? (Comment on purpose, related project, or other area of interest for which the report will be used.) _____

4. Specifically, how is the report being used? (Information source, design data, procedure, source of ideas, etc.) _____

5. Has the information in this report led to any quantitative savings as far as man-hours or dollars saved, operating costs avoided, or efficiencies achieved, etc? If so, please elaborate. _____

6. General Comments. What do you think should be changed to improve future reports? (Indicate changes to organization, technical content, format, etc.) _____

CURRENT
ADDRESS

Organization

Name

Street or P.O. Box No.

City, State, Zip Code

7. If indicating a Change of Address or Address Correction, please provide the Current or Correct address above and the Old or Incorrect address below.

OLD
ADDRESS

Organization

Name

Street or P.O. Box No.

City, State, Zip Code

(Remove this sheet, fold as indicated, tape closed, and mail.)
(DO NOT STAPLE)